Geotechnical Aspects of Underground Construction in Soft Ground, Kastner, Emeriault, Dias, Guilloux (eds)
 ISBN 2-9510416-3-2

Three-dimensional analysis of ground settlements due to tunnelling: Role of K_o and stiffness anisotropy

G. T. K. Lee & C. W. W. Ng
The Hong Kong University of Science and Technology, Hong Kong

ABSTRACT: Ground settlements due to tunnelling are three-dimensional (3D) in nature, especially at the tunnel heading. A series of 3D elasto-plastic coupled-consolidation finite element analyses has been conducted to investigate the effects of K_0 and stiffness anisotropy on ground settlements due to tunnelling.

1 INTRODUCTION

In recent years, the demand for tunnels is increasing worldwide. In each tunnelling project, an accurate and appropriate design is very important for excavating the tunnel safely and economically. With the advance of technology, 3D numerical simulations of complex soil-structure interactions become more and more feasible and economical in engineering practice. Over the years, many researchers have studied the influence of different soil models on surface settlements due to a tunnel excavation. Lee & Rowe (1989) conducted a series of two dimensional (2D) elastoplastic undrained finite element analyses to determine the effect of elastic anisotropy on surface settlements caused by tunnelling. They found out that the ratio of independent shear modulus to vertical modulus (G_{vh}/E_v) governs the shape of a settlement trough. By using a range of G_{vh}/E_v values from 0.2 to 0.25, they could produce a reasonable match between their computed results with the centrifuge model tests conducted in kaolin clay by Mair (1979). Theoretically, G_{vh}/E_v should be equal to 0.33 for the centrifuge model tunnel constructed in an isotropic ground under undrained conditions. Moreover, they found that soil stiffness anisotropy in terms of stiffness ratio and Poisson's ratio (i.e., $n = E_h/E_v < 1.5$ and $\nu_{hh} \neq \nu_{vh}$) does not greatly affect the ground settlement due to tunnelling. Addenbrooke (1996) conducted a series of comprehensive 2D (plane strain) numerical analyses of tunnelling in stiff clay with different pre-yield constitutive soil models (isotropic linear elastic, anisotropic linear elastic and isotropic non-linear elastic model) and different initial ground conditions (i.e., $K_0 = 0.5$ and $K_0 = 1.5$). Tunnels with 4.146m diameter excavated in London Clay at different depths (i.e., depth of tunnel axis, z_o = 20m, 29.3m and 34m) were modelled. In his undrained analyses, he showed that there was no significant difference between the isotropic and anisotropic cases regarding predicted ground movements around the tunnel with the use of anisotropic soil parameters ($G_{vh}/E_v' = 0.44$) given by Burland & Kalra (1986) for London clay. He also conducted a parametric study to investigate the effects of G_{vh} and n on surface settlements and concluded that by varying n with a constant G_{vh} the surface settlement profile was not greatly affected. On the other hand, a variation of G_{vh} has more significant influences on surface settlement with a constant n. The smaller the G_{vh} value, the deeper surface settlement trough will result. Moreover, by assuming a low K_0 zone around a 2D tunnel cross-section, he showed that a deep settlement trough could be reproduced by using a non-linear isotropic soil model and parameters.

Obviously, a tunnel excavation is truly three-dimensional (3D) in nature. In this paper. a series of 3D elasto-plastic coupled-consolidation analyses was conducted using the finite element method (FEM) to investigate the effects of K_0 and soil stiffness anisotropy (n) on ground surface settlement due to tunnelling. In the 3D numerical simulations, different K_0 values (i.e., 0.5 and 1.5) and soil stiffness anisotropy ratio ($n = E_h'/E_v' = 1.0$ for isotropic cases and n = 1.6 for anisotropic cases) were considered.

2 THREE-DIMENSIONAL NUMERICAL MODELLING

2.1 *Finite Element Mesh and Boundary Conditions*

In this 3D numerical study, a hypothetical tunnel excavation in a stiff homogenous overconsolidated London clay layer was modelled. The diameter of the tunnel (D) was taken as 9m and a constant cover depth (C) of 18m was assumed. The finite element program, ABAQUS (Hibbitt, Karlsson & Sorensen Inc., 1998), was used to model the tunnel excavation with coupled consolidation.

Figure 1 shows the finite element mesh adopted in the analysis. It should be noted that only half of the tunnel was analysed as a plane of symmetry could be readily identified at x = 0. The finite element mesh was 101.25m long, 45m high and 75m wide. It consisted of approximately 5040 elements and 5642 nodes. A section located at the middle of the mesh (i.e. at y = 0m, called monitoring section), was monitored during every stage of excavation and construction. Soil and shotcrete lining was modelled by eight-noded brick and four-noded shell elements, respectively.

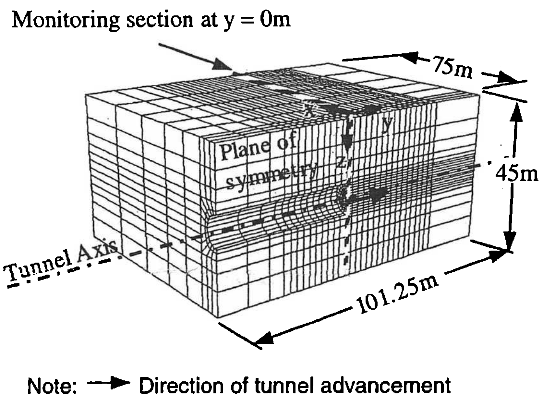

Figure 1. Three-dimensional finite element mesh.

Roller supports were applied on all vertical sides of the mesh while pin supports were assigned to the base of the mesh. Therefore, the movement in normal direction to all vertical sides of the mesh and the movements in all directions at the base of the mesh were restrained. The water table was assumed to be located at the ground surface.

2.2 *Constitutive Model, Model Parameters and Simulation Procedures*

An elastic-perfectly-plastic soil model governed by the Drucker-Prager failure criterion with a non-associated flow rule was used in this study. In all cases, the effective angle of friction (ϕ') was assumed to be 22° and the angle of dilation (ψ) was assumed to be 11°. The effective cohesion (c') was 5kPa. The soil stiffness parameters published by Burland & Kalra (1986) for the London clay at the New Queen Elizabeth II Conference Centre were adopted to simulate the clay layer. The variations of E_v' and E_h' were assumed to increase linearly with depth. The ratio of the independent shear modulus (G_{vh}) to the vertical effective Young's Modulus (E_v') was assumed to be 0.44 in all cases. The initial K_o conditions were assumed to be either 0.5 or 1.5. All the soil parameters used in this study are summarised in Table 1.

The tunnel lining was modelled as linear elastic material. The Young's modulus and Poisson's Ratio for the tunnel lining was taken to be 30×10^6kPa and 0.3, respectively. The unit weight of the shotcrete lining was 24kN/m^3.

An open face sequential tunnel excavation was modelled in this study. Tunnel excavation and construction were simulated by deactivating the soil elements within the proposed tunnel excavation zone at a rate of 2.25m/day. No support was applied on the tunnel face. A 250mm-thick shotcrete lining was applied on the tunnel wall at 2.25m (i.e., D/4) behind the tunnel face as the tunnel advances. This was done by activating the lining elements behind the unsupported span.

Table 1. Soil parameters used in the finite element analyses.

	n = 1.0	n = 1.6
E_v' (kPa)	12000+6240z	7500+3900z
E_h' (kPa)	12000+6240z	12000+6240z
$\nu_{vh}' = \nu_{hh}'$	0.125	0.125
G_{vh}/E_v'	0.44	0.44
ρ_d (kN/m^3)	15*	15*
e	1.0	1.0
k (m/s)	1×10^{-9}	1×10^{-9}
c' (kPa)	5	5
ϕ' (°)	22	22
ψ (°)	11	11

Note: z is the distance measured from the ground surface in meter.
* equivalent to saturated unit weight of 20 kN/m^3

3 COMPUTED RESULTS

3.1 *Transverse Ground Settlements*

As suggested by Peck (1969), measured transverse surface settlements in the field can be represented by a normal distribution or Gaussian distribution as follows:

$$S_x = S_{max} \exp(-x^2 / 2i^2) \tag{1}$$

where S_x is the transverse surface settlement; S_{max} is the maximum transverse surface settlement on the tunnel centreline; x is the transverse distance from the tunnel centreline and i is the point of inflection of the settlement trough. New and Bowers (1994) have reported measured values of S_{max} and i for oval-shaped tunnels excavated by the New Austrian Tunnelling Method (NATM) in London clay. The tunnel had a face area of about 59m^2 with an equivalent tunnel diameter of 8.7m and the depth of the tunnel axis (z_o) was located at approximately 21m below ground. The measured values of S_{max}/D and i/z_o ranged from 0.24% to 0.46% and from $0.35z_o$ to $0.48z_o$, respectively and volume losses lied between 1.1% and 1.4%. For shield tunnels constructed in London clay, Lake et al. (1992) reported that the measured values of S_{max}/D ranged from 0.10% to

0.17% and i/z_o lied between 0.45 and 0.52. The volume losses were ranging from 0.19% to 1.38% (based on reported S_{max} and i).

Figure 2 shows the normalised immediate transverse surface settlements induced at the monitoring section (at y = 0) when the tunnel face just reaches it. For the $K_0 = 0.5$ and n = 1.6 case, it gives the deepest settlement trough. The S_{max} is 0.18%D with $i/z_o = 0.44$ (Note that the i value was deduced from the numerical analysis). For the case with $K_0 = 0.5$ and n = 1.0, the S_{max} reduces to 0.09%D and i increases to $0.51z_o$ (see Table 2a). Obviously, n has significant influence on the magnitude and the shape of surface settlements. Since stress change due to tunnelling is governed by K_0 values only, irrespective n value used in the analysis. Thus, for a given K_0, the higher the n value, the smaller the ratio of the horizontal to vertical strain. This leads to a deeper settlement trough. Similar trends are also obtained for the K_0 = 1.5 cases.

On the other hand, for a given constant n = 1.6, the S_{max} reduces from 0.18%D (K_0 = 0.5 case) to 0.06%D (K_0 = 1.5 case) and i increases from $0.44z_o$ (K_0 = 0.5 case) to $0.58z_o$ (K_0 = 1.5 case). Similar trends are also obtained for n = 1.0 cases. It is clear that at a given K_0, the ground settlement trough becomes shallower and wider as n reduces from 1.6 to 1.0 whereas at a constant n, the ground settlement becomes shallower and wider as K_0 increases from 0.5 to 1.5. Although the effect of n on the magnitude of maximum surface settlements is more significant in the low K_0 case than that in the high K_0 case, the ratio of the maximum surface settlement computed in the n = 1.6 case to that in the n = 1.0 case is 2.65 and 1.96 for K_0 = 1.5 case and K_0 = 0.5 case, respectively.

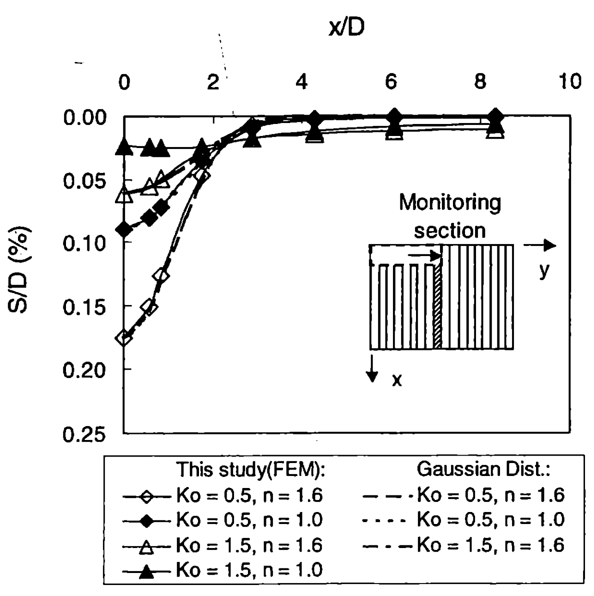

Figure 2. Immediate transverse surface settlements at the monitoring section (tunnel face at y = 0).

Based on the S_{max} and i deduced from each numerical analysis, a Gaussian distribution is fitted to the transverse surface settlement trough and plotted in Figure 2 for comparisons. It can be seen from the figure that immediate surface settlements can be represented by Gaussian distributions for the two K_0 = 0.5 cases (i.e., n = 1.6 and 1.0). Parameters obtained to describe the Gaussian distributions are given Table 2a. As K_0 increases, the discrepancy between the Gaussian distribution and the numerical prediction appears to be more significant at the remote boundary (away from the tunnel). For K_0 = 1.5 and n = 1.6 case, the numerical result gives a much wider settlement trough than the Gaussian distribution. In addition for the K_0 = 1.5 and n = 1.0 case, numerical predicted settlements do not show the form of a Gaussian distribution as the S_{max} does not occur at the tunnel centreline (i.e. at x/D = 0).

Table 2a – Summary of S_{max}, i and V_s for the immediate surface settlement troughs obtained from the numerical analyses.

	$K_0 = 0.5$		$K_0 = 1.5$	
n	1.6	1.0	1.6	1.0
S_{max}/D (%)	0.18	0.09	0.06	0.02
i/z_o	0.44	0.51	0.58	N/A
V_L (%)	0.64	0.41	0.46	0.31

Table 2b – Summary of S_{max}, i and V_s for the plane strain surface settlement troughs obtained from the numerical analyses.

	$K_0 = 0.5$		$K_0 = 1.5$	
n	1.6	1.0	1.6	1.0
S_{max}/D (%)	0.22	0.14	0.05	0.03
i/z_o	0.47	0.51	0.80	N/A
V_L (%)	0.84	0.61	0.56	0.38

Figure 3 shows the normalised transverse surface settlements at the monitoring section when the section reaches the plane strain condition (i.e., when the tunnel face advances to a distance at 3 times the tunnel diameter or more away from the monitoring section). Similar to the immediate surface settlements directly above the tunnel face, for a given K_0, the magnitude of plane strain surface settlements decreases with the n value. On the other hand, for a given n value, the magnitude of plane strain surface settlement decreases as K_0 increases.

The deduced S_{max}/D and i/z_o from the numerical analyses for the plane strain surface settlements are summarized in Table 2b. By comparing the deduced values and the field observations from shield tunnels reported by Lake et al. (1992), it is clear that computed results from the two analyses using K_0 = 0.5 are generally consistent with field measurements. However, this is not the case for predictions obtained from analyses using K_0 = 1.5.

Previous studies have revealed that G_{vh} has a significant effect on the depth of plane strain surface settlement (Simpson & Ng, 1995 and Addenbrooke, 1996). Using a smaller value of G_{vh} in an analysis will predict a deeper settlement trough. In the current study, G_{vh} is assumed to be a function of E_v' (i.e., $G_{vh}/E_v' = 0.44$). Since E_v' used in the n = 1.6 analysis is smaller (see Table 1) than that in n = 1.0 one, this results in a smaller value of G_{vh} in the former than that in the latter analysis. Therefore, for a given constant K_0, the plane strain surface settlements for n = 1.6 are deeper than those in the n = 1.0 cases (see in Figure 3). The same explanations are likely applicable to the immediate settlements shown in Figure 2.

In Figure 3, the results from a relevant two dimensional plane strain numerical study of tunnelling at 20m below ground (z_o = 20m) in London clay reported by Addenbrooke (1996) are also included for comparisons. The surface settlements shown are obtained from isotropic and anisotropic linear elastic analyses. Since the tunnel diameter and the depth of tunnel axis in the Addenbrooke's study (D = 4.146m, z_o = 20m) are different from this current study (D = 9m, z_o = 22.5m), only qualitative comparisons are possible. It can be seen from the figure that the general trends of the predicted settlement troughs from the Addenbrooke's and this study are consistent. Both sets of analyses show the importance of K_0 in predicting ground settlement profiles due to tunnelling. However, for a given K_0, it appears that the effects of n value on the depth of surface settlement trough in this study are far more significant than that in Addenbrooke's one. In his study, surface settlements were mainly governed by K_0, but were very little influenced by n value. This may be attributed to the undrained assumptions (i.e., constant volume) used in his study.

Moreover, the wider settlement troughs (for K_0 = 0.5 cases) obtained from the Addenbrooke's study than those from this study, may be attributed to different modelling techniques adopted in these two types of analyses. In the 2D plane strain analyses conducted by Addenbrooke, a prescribed volume loss was imposed in his analyses. The tunnel lining was applied to the tunnel wall until the prescribed volume loss (i.e., V_s = 1.3%) was reached. However, in this study, actual tunnel excavation sequence was closely simulated three-dimensionally. Soil elements were removed in the tunnel and lining was applied to the tunnel wall at a specific unsupported span behind the tunnel face. Therefore, it is not surprising to obtain different settlement profiles from different modelling techniques.

Due to the assumption of linear elastic soil stiffness within the yielding surface, the predicted volume losses in this study range from 0.38% to 0.84% (see Table 2b), which fall between measured values of 0.19% to 1.4% for shield tunnels constructed in London clay. However, the computed values are smaller than the measured ranges from 1.1% to 1.4% for tunnels constructed using the NATM in London clay. It is believed that the predicted volume loss will increase if soil stiffness is allowed to vary with strains within the yield surface. Also Tang (2001) demonstrated that volume loss in a 3D linear elastic analysis is proportional to the length of unsupported span. The longer the unsupported span assumed in an analysis, the larger the volume loss will be.

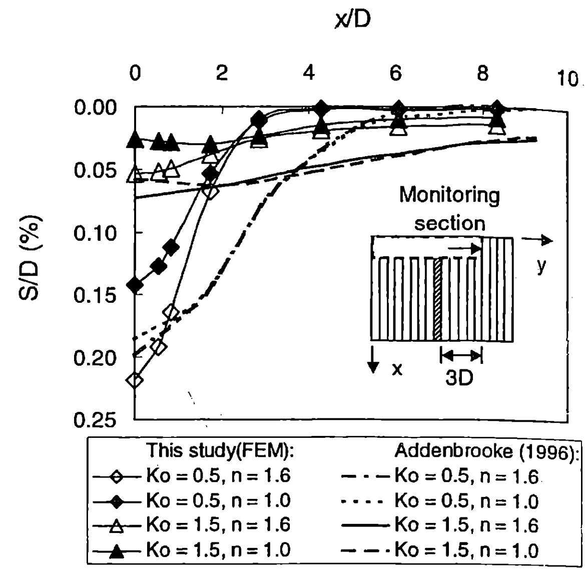

Figure 3. Plane strain transverse surface settlements at monitoring section (tunnel face at y = 3 times tunnel diameter ahead of the monitoring section).

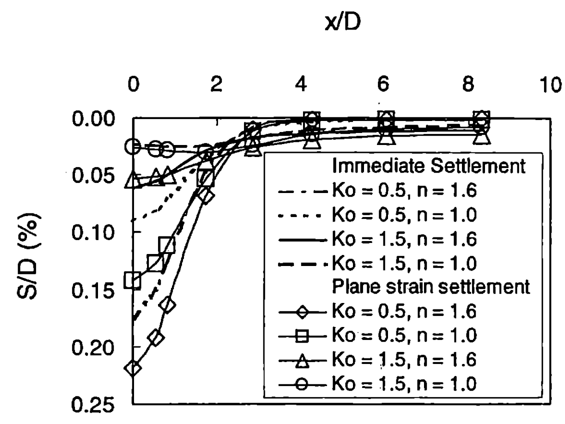

Figure 4. Immediate and plane strain transverse ground settlements.

Figure 4 shows the comparisons between normalised immediate and plane strain surface settlements obtained in the 3D analyses. For K_0 = 0.5, there is a significant increase in surface settlements at the monitoring section when the tunnel face advances from the monitoring section to a distance at three times of the tunnel diameter away from the monitoring section (i.e., the monitoring section reaches the plane strain conditions). The increased maximum settlement is about 22% and 56% for n = 1.6 and 1.0, respectively (refer to Table 2a and 2b). On the contrary, there is no major difference between the computed immediate and plane strain settlements for K_0 = 1.5. Due to the low water permeability in the clay, the increase in settlement for the low K_0 case cannot be mainly attributed by the dissipations of excess pore water pressure. In fact, the increase in settlement in the plane strain section is attributed to the significant increase in vertical effective stress beneath the invert. Relatively speaking, there is only a small increase in the vertical stress for the high K_0 case. Details of the 3D stress transfer mechanisms during the tunnel advancement are given by Ng & Lee (2003).

3.2 *Longitudinal Surface Settlements*

Attewell and Woodman (1982) studied a number of case histories of tunnel excavation in clays and they suggested a cumulative probability function for estimating longitudinal settlement profile due to tunnelling as follows:

$$S_y = \frac{V_s}{\sqrt{2\pi} i} \exp\frac{-x^2}{2i^2}\left[G\left(\frac{y-y_i}{i}\right) - G\left(\frac{y-y_f}{i}\right)\right] \quad (2)$$

where S_y is the longitudinal surface settlements; V_s is the volume of the transverse settlement trough per unit distance of tunnel advancement; x is the transverse distance from the tunnel centreline; i is the point of inflection of the settlement trough; y_i is the start point of tunnel; y_f is the final position of tunnel face, and probability function G is defined as

$$G(\alpha) = \frac{1}{\sqrt{2\pi}} \int_{-\infty}^{\alpha} \exp\frac{-\beta}{2} d\beta \quad (3)$$

the result of the above probability function can be obtained from standard probability tables.

Attewell & Woodman (1982) found that the immediate surface settlement directly above the tunnel face corresponds to about $0.5S_{max}$ (at the plane strain conditions) for tunnel constructed in stiff clays without face support. However, for tunnels excavated in soft clay with full-face support (e.g., shield tunnelling), the surface settlements are mainly caused by movements at the tail void. The immediate surface settlement directly above the tunnel face is considerably less than $0.5S_{max}$. Therefore, a translation of the cumulative probability function is required in order to match the field observation.

Figure 5 compares computed longitudinal settlements along the centreline of the tunnel (x = 0) by the numerical analyses and predictions using the cumulative probability function. For estimating the longitudinal surface settlements, values of V_s and i obtained from the numerical analyses are applied to the cumulative probability function. For K_0 = 0.5, the computed longitudinal surface settlements from the FEM analyses in the n = 1.6 case is deeper than the n = 1.0 case. The maximum computed settlement (S_{max}) does not appear at the tunnel heading (i.e., y/D = 0) but it occurs at the plane strain sections (i.e., at y/D = -3 or -4). On the contrary, the S_{max} occurs directly above the tunnel face for the two K_0 = 1.5 cases.

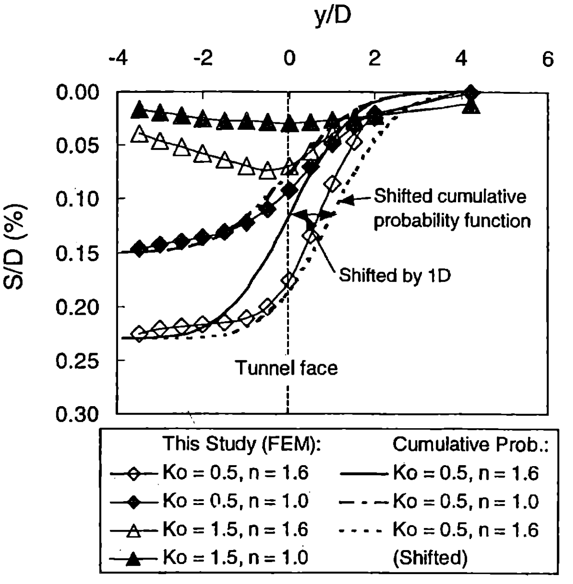

Figure 5. Longitudinal ground settlement along the tunnel centreline.

As shown in the figure, for K_0 = 0.5 (both n = 1.0 and n =1.6 cases), the cumulative probability function is compared with the longitudinal settlement troughs obtained from the numerical analyses. It can be seen that for the n = 1.0 case, the computed surface settlement directly above the tunnel face is approximately $0.5S_{max}$. Therefore, the numerical results can be represented by the cumulative probability function. On the other hand, for the n = 1.6 case, the anisotropic soil parameters give deeper surface settlement trough ahead of the tunnel face. The surface settlement directly above the tunnel face is approximately $0.8S_{max}$. The cumulative probability function is therefore required to shift ahead the tunnel face by one tunnel diameter in order to fit the computed results.

For the K_0 = 1.5 cases, the ground surface behind the tunnel face slightly heaves when the tunnel face reaches the monitoring section. Therefore, the longitudinal settlement troughs cannot be represented by the cumulative probability function.

4 CONCLUSIONS

Based on the 3D numerical simulations of the tunnel advancement at 2.25m/day (unsupported length), it is clear that surface ground settlements including immediate and plane strain settlements are governed by the combined effects of K_0 and anisotropic stiffness ratio, n. A combination of low K_0 condition with high degree of stiffness anisotropy will produce the deepest settlement trough. For the cases considered in this paper, it appears that the effects of K_0 are relatively more important than stiffness anisotropy on the calculations of ground settlements. Only under the low K_0 ground conditions, computed transverse and longitudinal settlements can be fitted well by empirical Gaussian distributions and Attewell and Woodman's cumulative probability functions, respectively.

By comparing the computed transverse immediate and plane strain settlements, it is found that there is a significant increase in surface settlements at the monitoring section under the low $K_0 = 0.5$ ground conditions. The increased maximum settlement at the monitoring section as the tunnel face advances from the monitoring section to a distance three times the tunnel diameter away are about 22% and 56% for n = 1.6 and 1.0, respectively. On the contrary, there is no major difference between the computed immediate and plane strain settlements for $K_0 = 1.5$.

ACKNOWLEDGEMENTS

This research project is supported by research grants HKUST714/96E provided by the Research Grants Council of the HKSAR and HIA96/97.EG03 of the Hong Kong University of Science and Technology.

REFERENCES

Addenbrooke, T. I. (1996). *Numerical Analysis of Tunnelling in Stiff Clay.* PhD Thesis, University of London (Imperial College of Science Technology and Medicine).

Attewell, P. B., and Woodman, J. P. (1982). Predicting the dynamics of ground settlement and its derivatives caused by tunnelling in soil. *Ground Engineering*, **15** (8): 13-20, 36.

Burland, J. B. & Kalra, J. C. (1986). Queen Elizabeth II Conference Centre: Geotechnical Aspects. *Proc. Instn. Civ. Engrs., Part1*, 80, Dec., 1479-1503.

Hibbitt, Karlsson & Sorensen Inc. (1998). ABAQUS *User's Manual, version 5.8.*

Lake, L. M., Rankin, W. J. and Hawley, J. (1992). Prediction and effects of gorund movements caused by tunnelling in soft ground beneath urban areas. *CIRIA Project Report* 30, Construction Industry Research and Inforamtion Association, London.

Lee, K. M. & Rowe, R. K. (1989). Deformations caused by surface loading and tunnelling: the role of elastic anisotropy. *Géotechnique*, **39**: 125-140.

Mair, R. J. (1979). *Centrifugal modelling of tunnel construction in soft clay.* PhD. Thesis, Cambridge University.

New, B. M. and Bowers, K. H. (1994). Ground movement model validation at the Heathrow Express trial tunnel. *Tunnelling 94*, Proc. 7th Int. Symposium of Ints. of Mining and Metallurgy and British Tunnelling Society, London, Chapman and Hall, 302-329.

Ng, C. W. W. & Lee, G. T. K. (2003). Three-dimensional stress transfer mechanisms due to tunnelling. (in preparation).

Peck, R. B. (1969) Deep excavation and tunnelling in soft ground. State of the Art Volume. *Proc. 7th International Conference on Soil Mechanics and Foundation Engineering*. 225-290.

Simpson, B. & Ng, C.W.W. (1995). Anisotropic analysis of settlement trough due to tunnelling in an overconsolidated clay. *Proc. 10th Asian Regional Conf. on Soil Mech. & Fdn. Engng, Beijing*, Vol. 2. 166-167.

Tang, K. W. D. (2001). *Numerical studies of multiple NATM tunnel interaction in soft ground.* MPhil. Thesis, The Hong Kong University of Science and Technology.

APPENDIX I. NOTATIONS

C	Cover depth
c'	Effective cohesion
D	Tunnel diameter
E_h'	Horizontal effective Young's modulus of soil
E_v'	Vertical effective Young's modulus of soil
G_{vh}	Independent shear modulus
i	Point of inflection of the settlement trough
k	Coefficient permeability of soil
K_0	Coefficient of earth pressure at rest
n	Ratio of horizontal effective Young's modulus to vertical effective Young's modulus of soil
S_{max}	Maximum surface settlement
S_x	Transverse surface settlement
S_y	Longitudinal ground settlement
V_L	Volume of ground loss expressed as a fraction of the tunnel area
V_s	Volume of the transverse settlement trough per unit distance of tunnel advancement
x	Horizontal distance from tunnel centreline
y	Horizontal distance measured in the longitudinal direction
y_i	Start point of tunnel
y_f	Final position of tunnel face
z	Depth measured from ground surface
z_o	Depth of tunnel axis
ϕ'	Effective angle of friction
ν_{vh}'	Effective Poisson's ratio for the effect of vertical stress on horizontal strain
ν_{hh}'	Effective Poisson's ratio for the effect of horizontal stress on horizontal strain
ρ_d	Dry density
ψ	Angle of dilation